IMPROVING LASER MANUFACTURING PROCESSES BY MEANS OF MULTIPHYSICS SIMULATIONS

RODRIGO GÓMEZ VÁZQUEZ
Vienna University of Technology
ANDREAS OTTO
Vienna University of Technology

ABSTRACT

In this paper we present an example of how laser manufacturing technology can benefit from the use of realistic process simulations. The general design of the multiphysical model used allows for the simulation of different kinds of laser processes such as welding, cutting or more recently even ultra-short pulse ablation [1]. The model is able to perform the simulation of the complete process, thus providing useful technical information such as the influence of keyhole front inclination or of surface tension on the flow of the molten material and its consequences after the solidification. In addition to the implementation of physical models, the current ongoing work presented is aimed to improve the simulation performance in massively parallel scenarios such as HPC-clusters or cloud environments, because the increasing availability of these resources shall eventually enable the application of expensive numerical calculations for production purposes.

Key words: *laser welding, Multiphysics, optimization, virtual process*

INTRODUCTION

The industrial implementation of laser assisted processing technologies is nowadays well-established due to the unique combination of accuracy, productivity and adaptability that laser sources permit. As laser assisted techniques allow for precisely controlling the thermal heat input it is possible e.g. to produce high-end components with a minimum influence on the functional characteristics. On the other hand, finding optimal process parameters is often a difficult task which involves the use of experimental methods that not always provide enough relevant process information. In this regard numerical simulations can help to fill this gap with the use of multiphysical models.

In contrast to other manufacturing technologies e.g. forming, the simulation of the process prior to its implementation is in the scope of laser assisted technologies not an obvious intermediate step in the production procedure. Indeed the current state of the art in the simulation of laser assisted processes does not allow a generalized use for industrial applications.

The complexity of the phenomena involved (e.g. processes involving plasma, melt ejections, etc.) demands the use of complex physical models. This means already a big effort in order to create a model that combines all those physics in a coupled manner and in some cases even the existing physical models are missing or not yet completely understood e.g. ultra-short pulse interaction phenomena. Furthermore, these simulations usually involve a very high computational demand due to the amount of different physical phenomena that must be calculated.

In order to overcome the existing gap between the state of the art in simulation of laser processes and the industrial demands it is necessary to work simultaneously on the improvement of the physics implementation as well as on the calculation performance.

The aim of this paper is to show the potential applications of these complex simulations for existing laser assisted processes as well as to provide an overview on the current ongoing work aimed to reduce their runtime.

DESCRIPTION OF THE SIMULATION MODEL

The simulation environment used is OpenFOAM® [2]. This software is an open source package suitable for the simulation of continuum physics on a Finite Volume approach that is used to solve systems of partial differential equations. It contains the necessary libraries for parallel calculations and though there are many solvers for general

CFD-applications available, the programing syntax adopted allows for convenient implementation of more specific physical models on their top.

Due to the characteristics of our field of application, we started from a solver called *multiphaseInterDyMFoam*, which is designed for the simulation of turbulent incompressible isothermal multiphase segregated flows with automatic re-meshing operations. It makes use of a Volume of Fluid formulation conveniently extended to deal with an unlimited number of phases. It must be emphasized that the concept of "phase" employed here is not equivalent to "material". Thus it is possible to define different phases of a same material in a simulation, each one having its own physical properties e.g. for solid and liquid state. The concept of phase-mixture is used to average the physical properties at every mesh cell, taking into account either the volume- or the mass-fraction of the phases present in each cell (depending on the physical meaning of the property being evaluated).

Several changes aimed to enhance the capabilities of the standard solver in order to simulate laser manufacturing processes in general were accomplished. Here we will only summarize the main of them:

The propagation of the laser intensity is modelled using a differential form of the radiative transfer equation. This approach takes into account partial attenuation due to semi-transparent media such as plasma, but it is not suitable for the calculation of multiple reflections. Therefore a ray tracing method that accounts for this effect is coupled right after the 1st incidence occurs. The angle of incidence determines the reflectivity according to Fresnel equations. Instead of coupling the absorbed energy directly in the energy conservation equation we place this source term in the electron side of a two-temperature model. The energy is initially absorbed by the electrons and only then transferred to the lattice by means of a coupling function until a thermal equilibrium between electrons and lattice is reached (see details in [3]). This procedure does not alter the results of conventional laser processes such as welding or cutting and it is of crucial importance for the simulation of ultra-short pulse ablation processes. An enthalpy-based energy conservation equation allows the calculation of heat transfer, which eventually leads to a greater or lesser extent into phase changes. At least solid, liquid and vapor states shall be defined as independent phases for each material. The phases and energy available inside a certain mesh element determine the magnitude of the phase change. For melting and solidification this implementation is similar to the one presented in [4]. Unfortunately this is not possible for the case of evaporation and condensation. We apply Clapeyron model for these phase changes, which does not only depend on the latent heat, but also on the temperature and on the local pressure. In many times we use an ideal-gas approach to calculate the properties of the vapor phases. The specific volume is temperature- as well as pressure-dependent, what means that the amount of vaporizing mass influences the local pressure and thus the phase change itself too. For this reason, these phase changes demand an additional iteration step. In order to avoid unphysically high velocities arising from the sudden expansion from condensed to gaseous state a compression model which deals with the concept of relative densities has been implemented (see details in [5]). Restriction of solid-phases movement is imposed by introducing a suitable source term into the equation of momentum conservation and the surface tension model was modified to account for surface tangential forces instead of normal ones, which is essential to resolve thermo-capillary driven meltpool flows.

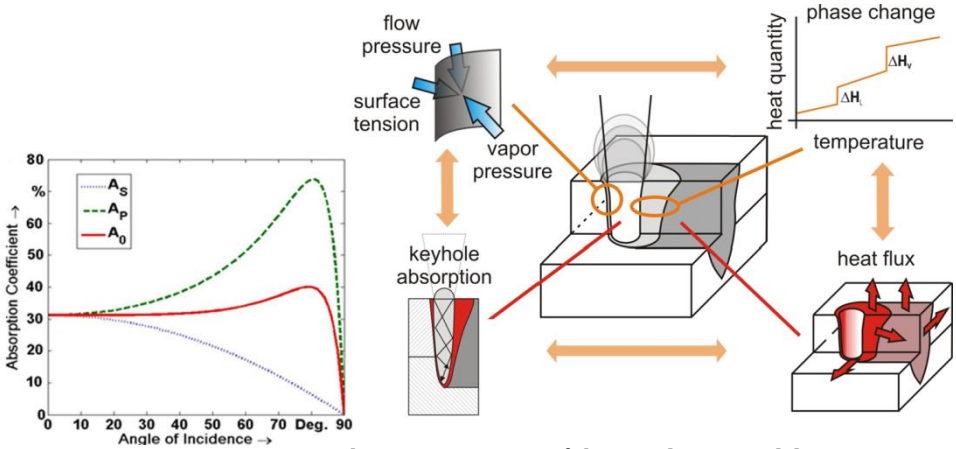

Fig. 1. Schematic summary of the simulation model.

The main conception of the simulation model consists on coupling physical laws, mostly implemented in form of differential equations, instead of simply using empirical models designed to describe specific cases. This general design is the key that makes possible the study of a wide range of conditions without substantial changes. Furthermore, the simultaneous solution of the numerous physics involved provides valuable information for the in-depth study of processes e.g. problems, causes and possible optimizing strategies.

EXEMPLARY APPLICATION: STUDY OF HUMPING FAILURES IN LASER WELDING

As above mentioned, the universal design of the model becomes advantageous for its use in process analysis. In this example the goal was to understand the physical mechanisms behind the so-called humping phenomenon. A deep understanding of the root causes shall allow a more efficient planning of the actions to take in order to optimize the process.

Humps are characteristic drop-like shapes that appear with certain intermittence on the top of a weld bead when operating at high feed rates (see Fig. 2). They have been observed over the last 50 years and though different approaches have been suggested up to now none of them could fully explain the occurrence of this phenomenon. This work is part of a common study between the Ernst-Abe-University of Applied Science in Jena (Germany) and our group at the Technical University of Vienna (Austria). More details about this study can be found in [6]. For this analysis we chose a set of conditions that evidenced humping behavior in the experimental tests of laser micro welding. These are presented in the Table 1.

Table 1. Studied conditions for laser micro welding [6].

Workpiece material	Foil thickness	Wavelength	Power	Spot size	Feed rate
Stainless steel	100 µm	1,07 µm	400 W	25 µm and 65 µm	1.2 m/s

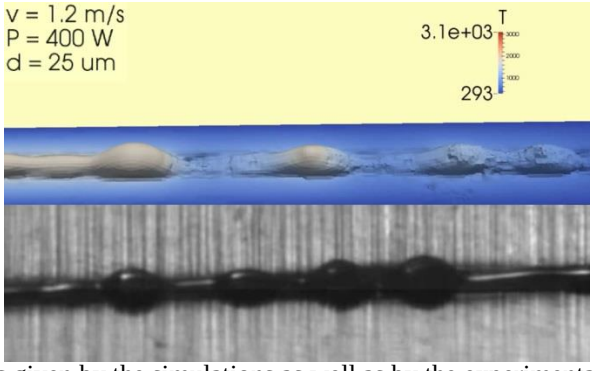

Fig. 2. Hump structures given by the simulations as well as by the experimental test with the spot size of 25µm.

Fig. 3 shows a descriptive view of the main areas involved in the process of hump formation. The most decisive one is the absorption front, whose angle directly relates to the feed rate applied. In this zone is where the species evaporation takes place. Thus the direction of the resulting vapor flow is originally normal to the absorption front. In addition, the recoil pressure, which also acts normally to the front, forces the molten material to flow away laterally, from where it continues flowing backwards along the walls of the elongated keyhole. This is result of the high pressure induced by the vaporizing process at the front. The initial upwards component of this flow due to the combined effect of the vapor flow drag forces and of the front pressing (both perpendicular to the front) can be appreciated from the scheme given in Fig. 3. At the precise conditions leading into humping this component does not reach to override the cohesive effect of the surface tension forces and to release spatter ejections, but is high enough to produce an upwards melt stream. Furthermore, the heat is also transported upwards along with the liquid stream, thus inducing faster solidification at the lower part of the foil. The side streams eventually create bridges at the rear part of the opened keyhole, where the magnitude of the recoil pressure is much lower than at the front. The melt solidifies starting from the bottom ant it creates a ramp-like front along which the forthcoming molten material will be conducted to flow up to the top of the foil. In addition there is an accumulation of the melt at the rear instead of a homogeneous spreading due to the effect of surface tension. These two phenomena amplify each other: on the one hand the ramped solidification front directs the melt upwards and on the other hand the upwards solidification gets more pronounced due to the heat accumulation at the top brought by the melt species. With the further advance of the solidification front the feedline of the hump finally gets constricted and the hump solidifies, leaving that characteristic droplet-like shape. Once leaving the hump behind, the solidification ramp recovers its initial inclination and the cycle starts again. Fig.4 shows different stages of this process.

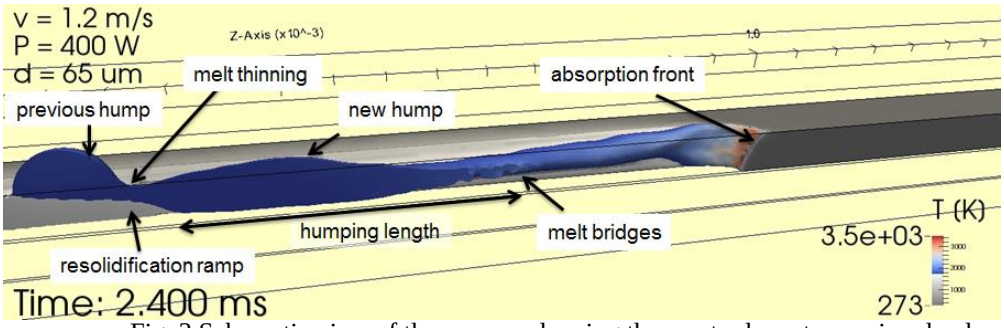

Fig. 3 Schematic view of the process showing the most relevant areas involved.

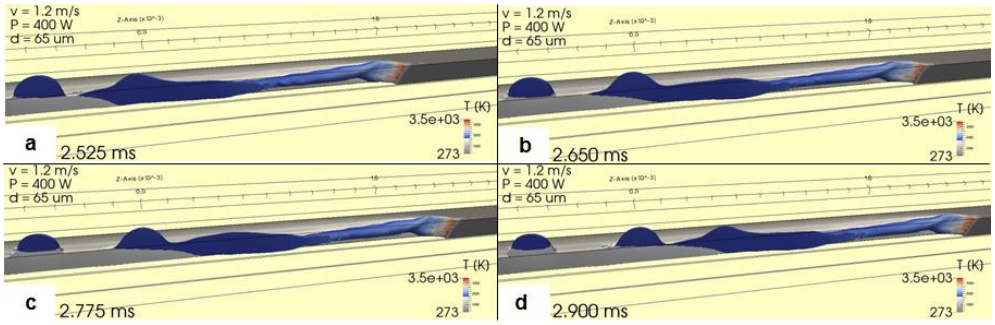

Fig. 4 Different stages of the hump formation in the course of the micro welding process.

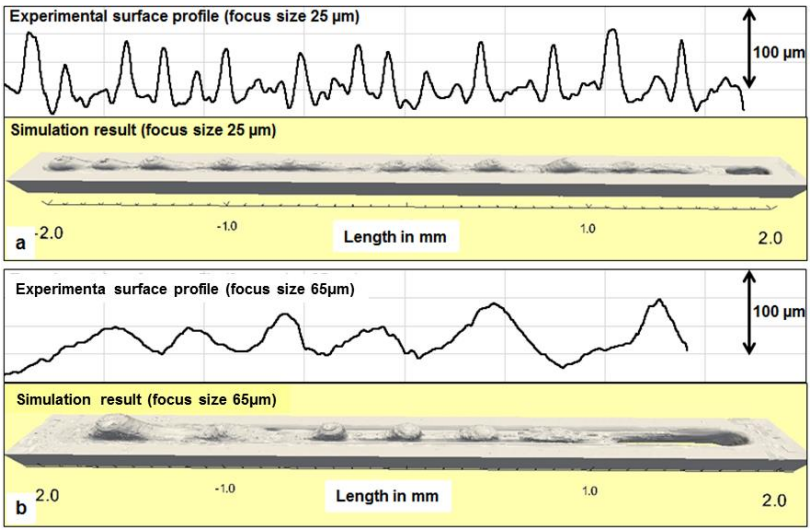

Fig. 5 Comparison between simulation results and experimental ones with the spot size of 25 µm and 65µm, respectively.

In a qualitative assessment we observe that the frequency of the humps seems to be related with the distance between the solidification front and the melt bridges, what we call “humping length”, as well as with the length of the elongated keyhole (see Fig. 3). The shorter these two distances are the higher hump frequency can be expected. Also in this aspect the simulation results were in good agreement with the experiments, as seen in Figure 5. In addition these distances increase when using bigger spot sizes, mainly because of the broader offset between the sides of the elongated keyhole and to the higher amount of melt produced.

The detailed description of the process mechanisms given by the simulations allowed to identify the inclination of the absorption front as the main control parameter in order to avoid the appearance of humping failures.

PERFORMANCE IN PARALLEL

One usual requirement for the process simulations is a reasonable calculation time, especially when the results are needed to support decisions within an industrial scope. On the other hand, the solution of multiphysical problems

inherently involves a huge calculation demand. For this reason is important to work with a code that allows high-scale parallel computing.

In general, OpenFOAM software allows excellent performance scaling in parallel environments. The performance rises almost linearly with the number of cores up to reference levels of around 10-20 thousand cells per core. While developing our solver on the top of it we tried to avoid non-parallelizable code as much as possible and thanks to that we are able to reach similar parallel performance marks in our benchmark tests as shown in Fig. 6.

One of the key features that allow whole process scale simulations is the use of Adaptive Mesh Refinement (AMR) techniques. These are already within the simulation software and allow refining regions basing on pre-defined parameters. For instance, while having a coarse background mesh for the workpiece and the surrounding medium, one may want to have a higher resolution at the meltpool in order to get a good description of the flow patterns and a higher one of the angle dependent absorption at the exposed surface (see Fig. 8 (a)). The fact that these regions are in continuous evolution implies that so does the mesh refinement. For single core simulations this approach allows the most efficient calculation. However, in parallel scenarios it is not necessarily the case.

When preparing a simulation in parallel the simulation domain gets divided in a more simple or complex geometrical way and each parallel process is in charge of the simulation of its own part of the original domain. In the course of the simulation and due to the continuous changes in the regions that must be re-meshed, some of the processes will end up having higher amount of cells than others (see Fig. 7). That leads to an unbalanced calculation where the bottleneck is set by the process with the highest load (typically the amount of cells). Other approaches like setting a pre-established refined mesh where the regions of interest are supposed to be is often a risky assumption and also inefficient, because it leads to an overall higher amount of cells. On the other hand the use of highly parallelized environments such as cloud computing services or dedicated HPC-cluster centers involves an economical investment. Therefore it is of main importance to use these resources as efficient as possible and that requires a more sophisticated calculation approach.

With this aim we recently coupled our model with a tool that allows for load balancing during the runtime. If the load imbalance among processes during the simulation exceeds at any time a predefined threshold value a redistribution of the simulation domain among the processes takes place in order to ensure a continuously quassi-balanced run and therefore an efficient use of the available hardware resources. Fig. 8 (b) shows the performance comparison of a benchmark test where the same case was simulated using 16 cores on a single node with three different approaches: a constant pre-refined grid of about 6.5 millions of elements in the regions where high resolution demand was expected (different from the one above mentioned); two grids with automatic AMR, one with invariant process distribution and the other one with automatic load balancing, both ending up with about 2.6 millions of elements.

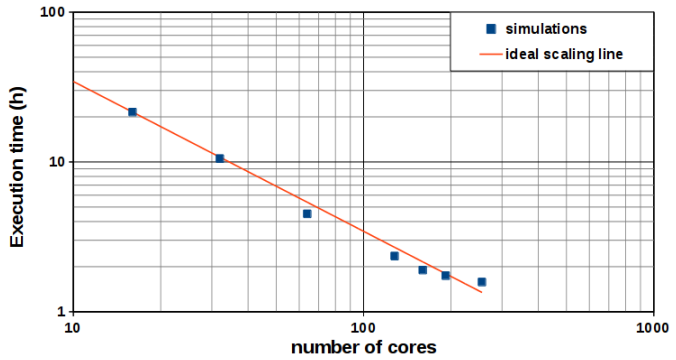

Fig. 6. Simulation performance in parallel for a benchmark case with a fixed grid of about 4 million of elements. The red line indicates the ideal trend where the simulation time decreases linearly with the number of cores used. The beginning of the stagnation area shows up at a level of exactly 20 thousand cells per core when using 192 cores.

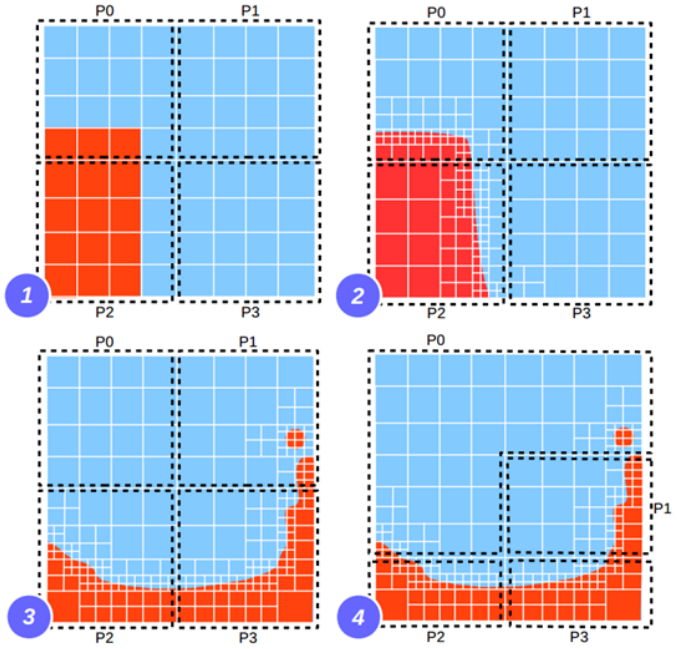

Fig. 7. Schematic evolution of the workload distribution in a parallel simulation with adaptive mesh refinement. The dotted lines represent the subdomains assigned to each of the processors. One can see how an initially well-balanced simulation (1st snapthot) gets unbalanced in the course of the run due to the successive mesh refinements that are performed automatically in order to keep a fine discretization at the fluid interface in this case (2nd and 3rd snapshots). A load balancing technique allows to redistribute the sub-domains in such a way that each processor ends up with a similar amount of mesh elements than the others (4th snapshot). For obvious reasons this shall be performed automatically during the runtime as well in order to maximize the computational efficiency.

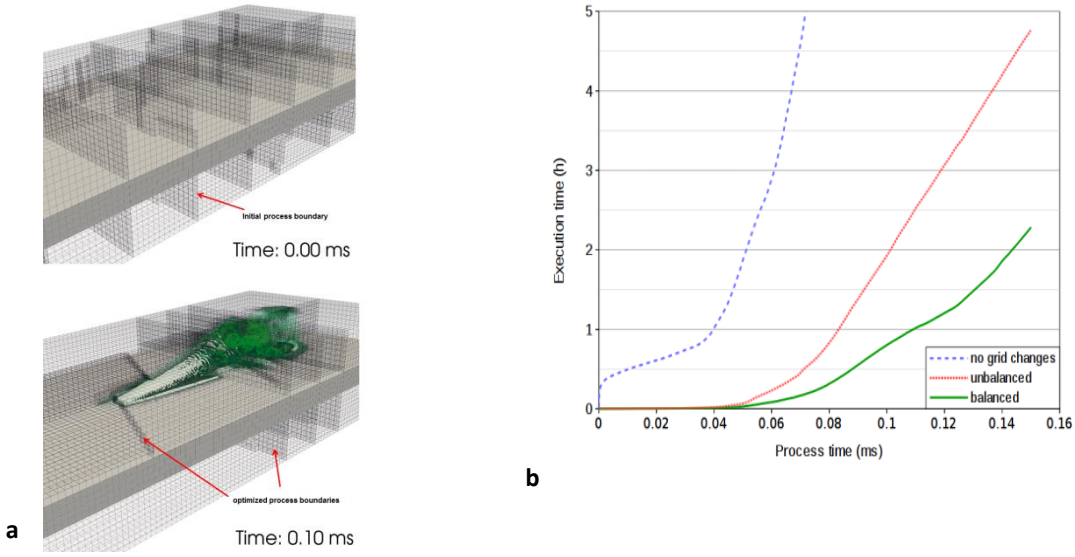

Fig. 8. (a) Above: Initial simulation domain showing the process boundaries. Below: Refined grid with balanced process distribution at a certain time during the simulation. Note that processor boundaries moved towards the refined regions as expected in order to compensate the originated imbalance. (b) Execution time in hours for each of the three simulations. The time saving increase continuously over the course of the simulation. Though not fitting in the plot scale, the total execution time for the case with fixed mesh was slightly higher than 24 hours.

SUMMARY AND OUTLOOK

In this work we showed the potential benefit of the use of multiphysical simulations for the laser assisted technologies, as well as the current limitations. In the forthcoming years, the maturity of the physical models along with the increased availability of massive parallel environments such as cloud services shall be the key to enable the integration of process simulations within the industrial production.

ACKNOWLEDGEMENTS

The authors would like to show their gratitude to their cooperation partners from the Ernst-Abe-University of Applied Science, as well as to the center for high-performance computation Vienna Scientific Cluster for the support provided in the course of this work.

REFERENCES

[1] Otto et al.: "Numerical Simulations - A Versatile Approach for Better Understanding Dynamics in Laser Material Processing", Physics Procedia A, 12, 11-20 (2011) http://dx.doi.org/10.1016/j.phpro.2011.03.003

[2] https://openfoam.org/

[3] Tatra et al.: "Numerical Simulation of Laser Ablation with Short and Ultra-short Pulses for Metals and Semiconductors", Physics Procedia, 83, 1339-1346 (2016) https://doi.org/10.1016/j.phpro.2016.08.141

[4] Voller et al.: "An enthalpy method for convection/diffusion phase change", International Journal for Numerical Methods in Engineering, 24 (1), 271-284 (1987) http://dx.doi.org/10.1002/nme.1620240119

[5] Otto et al.: "Multiphysical Simulation of ns-Laser Ablation of Multi-material LED-structures", Physics Procedia, 56, 1315-1324 https://doi.org/10.1016/j.phpro.2014.08.057

[6] Otto et al.: "Numerical and Experimental Investigations of Humping Phenomena in Laser Micro Welding", Physics Procedia, 83, 1415-1423 (2016) https://doi.org/10.1016/j.phpro.2016.09.004